Depolarized light scattering from fractal soot aggregates

N. Lu and C. M. Sorensen
Department of Physics, Kansas State University, Manhattan, Kansas 66506-2601
(Received 25 April 1994)

We have measured the depolarization ratio ρ of light scattered from three different premixed hydrocarbon-oxygen flames. The soot clusters in these flames are well described as fractals with a dimension of 1.79 ± 0.10. We show that the depolarization is due to intracluster multiple scattering. We also show that $\rho\sim N^{-0.6}$, where N is the number of monomers per cluster for scattering in the forward direction. We created simulated diffusion-limited-cluster-aggregate clusters on a computer and used a self-consistent electric-dipole-induced-dipole calculation to calculate ρ and again find $\rho\sim N^{-0.6}$. The calculated magnitude, however, is too small; various modifications are tried or suggested to bring about a quantitative agreement of theory and experiment.

PACS number(s): 42.25.Fx, 78.20.Dj, 82.70.Rr

I. INTRODUCTION

Experiments involving the scattering of waves from fractal aggregates have contributed significantly to our understanding of these aggregates and the processes by which they are made [1]. More specifically, the optics of fractal aggregates has been of interest lately not only because of its use as an *in situ* diagnostic of aggregate size and morphology [2–7], but also because of its importance to other concerns such as air pollution and visibility problems and the nuclear winter scenario [8,9], radiative transfer in flames [10], and interplanetary, interstellar, and cometary dust scattering problems [11].

When considering the interaction of light with aggregates, it is usually assumed that only single scattering occurs, but it is well acknowledged that multiple scattering has a finite probability and this probability increases with cluster size and number density. Questions naturally arise concerning the extent of multiple scattering, whether it is due to inter- or intracluster scattering, and how analysis of scattering data must be modified to account for its presence. This last point is important if light scattering is to remain a viable diagnostic for *in situ* measurements. Another reason for studying multiple scattering is because it appears to be sensitive to higher-order structure in the cluster than that describable by the fractal dimension and hence may allow quantification and measurement of such structure [12,13]. Finally, it is conceivable that it will be sensitive to other cluster parameters such as shape and refractive index and hence may lead to methods by which such parameters may be measured.

The history of the optical multiple scattering problem is extensive [14–18]. In general, all the various treatments involve a self-consistent coupling of the electromagnetic waves between the scatterers. Differences occur in how the coupling interactions are approximated, how the self-consistency is terminated, or how the individual scatters are geometrically arranged. With regard to this last point, the realization that many naturally occurring aggregates can be quantitatively described as fractals [19] has afforded a new perspective for studying the intracluster multiple scattering. Chen *et al.* [17] studied intracluster multiple scattering from colloidal gold fractal aggregates using a self-consistent field method. Their results showed that the effect of dipolar interactions simply changed the mean field refractive index of the particles whereas higher-order multipole interactions caused absorption resonances in the metallic particles. Frey *et al.* [18] considered just electric dipole interactions in simulated sootlike clusters of various fractal dimensions. They truncated the electric dipole tensor at the second-order term. With this, they calculated scattering of both polarizations and the depolarization ratio, and some of their results are similar to what we will report below.

In this paper we study the depolarization of light scattered by soot fractal aggregates in various premixed hydrocarbon-oxygen flames. This is quantified by the depolarization intensity ratio $\rho=I_{VH}/I_{VV}$, where the first subscript refers to the incident polarization and the second to the detected polarization, either horizontal or vertical. We show that the depolarization is due to intracluster multiple scattering. We also show for scattering in the forward direction that $\rho-N^{-0.6}$, where N is the number of monomers in the fractal aggregate, which was measured with a new, *in situ* optical technique [5]. By considering an electric-dipole-induced-dipole intracluster scattering mechanism, we make qualitative arguments regarding the experimental results. Then to obtain a quantitative description we create diffusion-limited-cluster-aggregate (DLCA) clusters with a computer simulation and perform a self-consistent electric-dipole-induced-dipole calculation. We successfully reproduce the $\rho-N^{-0.6}$ dependence, but find that the magnitude of ρ is very sensitive to a number of issues including approximating the monomers as point dipole scatterers, necking between monomers and the soot refractive index.

II. EXPERIMENTAL METHOD

The soot aerosol was created in premixed hydrocarbon-oxygen flames with methane, ethylene, and

propane. The burner and light scattering apparatus were similar to that used previously [4–7]. The flame was supported on a cooled porous frit burner obtained from McKenna Products. The premixed gases passed through the 5-cm-diam frit at a velocity of 6 cm/sec. This frit was surrounded by an annular sheath region 0.5 cm wide through which nitrogen gas flowed at 5 cm/sec. A 15-cm-diam steel stagnation plate was placed 3.0 cm above the burner surface to stabilize the flame. Fuel oxidizer ratios designated by the atomic carbon to oxygen ratios where C:O=0.75 for methane, C:O=1.1 for ethylene, and C:O=1.4 for propane flames. The arrangement yielded a quasi-one-dimensional flame with height above burner the only major variable. Past work has shown that the major growth mode of the soot clusters is aggregation. Thus the average number of monomers per cluster increases with height above burner. The fractal dimension is $D_f=1.79\pm0.10$. This fractal dimension, the overall physical appearance, and the manner in which they form all support the view that the soot clusters are well described as diffusion-limited cluster aggregates.

The light scattering apparatus used an argon ion laser operating at $\lambda=488$ nm. The beam was chopped and then focused into the flame by a 50-cm focal length lens. The scattering plane was horizontal and the incident beam passed through a Glan-Thompson polarizer with a vertical polarization axis. The scattered light was collected by another lens and the scattering volume imaged onto an adjustable iris. Next came another Glan-Thompson polarizer with a rotatable polarization axis so that either vertically or horizontally polarized light could be detected. The light then passed through an interference filter to pass only the 488-nm scattered light and then on to the photomultiplier tube (PMT). Scattered light could be detected at scattering angles θ between 5° and 110°. The output of the PMT was fed to an Oriel radiometer, which monitored the chopper and used phase sensitive detection to determine the scattered light intensity.

Two types of static light scattering experiments were performed on each flame. The first used a combination of static structure factor and absolute scattering and extinction measurements to characterize the morphology of the soot aggregates. This is a technique [5] which allows for an *in situ* measurement of the cluster radius of gyration R_g, fractal dimension D_f, number of monomers per aggregate N, and monomer radius a.

The basic ideas to the method are as follows. The structure factor, scattered intensity versus wave vector $q=4\pi\lambda^{-1}\sin\theta/2$, yields R_g in the small qR_g limit through a Guinier analysis as

$$I(q)=I(0)(1-q^2R_g^2/3) . \tag{1}$$

Once R_g is determined, D_f is obtained by a fit to the complete structure factor good for all qR_g. We write $I(q)=I(0)S(x)$, where $x=qR_g$ and

$$S(x)=e^{-x^2/D_f}\,{}_1F_1\left[\frac{3-D_f}{2},\frac{3}{2};\frac{x^2}{D_f}\right] \tag{2}$$

is the static structure factor. This form for $S(x)$ results for a Gaussian cutoff of the density autocorrelation function, which we have shown [6] to be more accurate than the often used exponential cutoff.

Additional information can be obtained from a scattering-extinction measurement [12]. The absolute scattered intensity is measured in the small qR_g regime by calibration of the scattering from the soot against that from gases of known Rayleigh ratio. A second PMT placed at $\theta=0°$ is used to measure the turbidity or extinction of the flame. Since scattering goes as nN^2a^6, where n is the cluster number density, and turbidity goes as nNa^3, their ratio yields a volume equivalent, so-called scattering-extinction radius

$$R_{SE}=aN^{1/3} . \tag{3}$$

This analysis requires a value for the soot refractive index, which we take as $m=1.6-0.6i$ [20,21].

To determine the morphological parameters we use

$$N=k_0(R_g/a)^{D_f} . \tag{4}$$

We have found $k_0=1.2\pm0.1$ for DLCA clusters [22]. Thus if light scattering measures R_g, D_f, and R_{SE}, then Eqs. (3) and (4) allow us to solve for N and a. We have shown this method yields results consistent with electron microscopy [7].

This method yields N and a under the assumption that the clusters are monodisperse, i.e., are of single size N. In fact, a size distribution exists described by $n(N)$, the number of clusters per unit volume with N monomers per cluster. Aggregation kinetics leads to a self-preserving or scaling form for $n(N)$ [23]

$$n(N)=M_1s_1^{-2}\phi(x) , \tag{5a}$$

$$x=N/s_1 , \tag{5b}$$

$$s_1=M_1/M_0 , \tag{5c}$$

and

$$\phi(x)=Ax^{-\tau}e^{-\alpha x} , \tag{5d}$$

where $A=\alpha^{\alpha}\Gamma^{-1}(\alpha)$, $\alpha=1-\tau$, and Γ is the gamma function. We also define $M_i=\int N^i n(N)dN$, the ith moment of the size distribution, and a mean cluster size $s_1=\langle N\rangle$. We have shown [5] that this distribution is better than the often used lognormal distributions for interpreting light scattering data which involve moments of the distribution higher than the second. We have also shown [5] how the a and N values determined under the monodisperse assumption above must be corrected for a finite distribution and we use that procedure with $\tau=0$ in our analysis to follow.

The depolarization ratio measurements were straightforward. With the detecting polarizer axis vertical, the I_{VV} intensity was measured; with it horizontal, I_{VH} was measured. The I_{VH} measurement involved adjusting the polarization axis through a few steps of a few tenths of a degree each to find the minimum in the scattered light which is the true I_{VH}. These measurements were performed at $\theta=20°$ so that $qR_g\ll1$ and hence $I_{VV}\sim N^2$.

III. RESULTS

At $\theta=20°$ all flames showed depolarization ratios of a few tenths to 1%, which decreased with increasing height above burner. The question is, what is this depolarization due to? Fluorescence from polycyclic aromatic hydrocarbons is a possible source of depolarized intensity and could be the source of the finite values of ρ [24]. Fluorescence is largest near the flame front (reaction zone), which for our flames was near $h\sim 0.6$ and ~ 0.1 cm wide. Our measurements were performed at $h\geq 1.0$ cm, where scattering is typically many orders of magnitude greater. This fact was confirmed when we used $\lambda=488$ nm for the incident beam and attempted to detect scattered radiation at 514.5 nm. The intensity at this wavelength was $\sim 10^5$ smaller than at 488 nm. Also in our depolarization experiments we detected the scattered light at the incident wavelength ($\lambda=488$ nm) far away from any expected peak in the fluorescence. Thus we conclude that fluorescence is not a factor.

Other sources of depolarization are multiple scattering and particle anisotropy [25]. Multiple scattering can be between different clusters, intercluster multiple scattering, or within single clusters, intracluster multiple scattering. A number of simple functional dependences have led us to conclude that the depolarization cannot be due to intercluster multiple scattering.

Intercluster scattering is an extrinsic effect dependent on the total number of clusters contributing to the signal. Intracluster multiple scattering and anisotropy are intrinsic depending only on single cluster properties. Therefore intercluster scattering depends linearly on the size of the scattering volume, the other mechanisms do not [15]. We varied our scattering volume size by a factor of 4 by changing the iris size in the detection optics and saw no change in the depolarization.

To lowest order the scattering of light is governed by the electric dipole tensor [15]. The electric field at $\mathbf{r}_2$ due to an oscillating dipole $\mathbf{p}$ at $\mathbf{r}_1$ is given by

$$\mathbf{E}(r_2)=k^2\overleftrightarrow{\mathbf{T}}(\mathbf{r}_{21})\cdot\mathbf{p}(\mathbf{r}_1)\ , \tag{6}$$

where $k=2\pi/\lambda$ and the electric dipole tensor is given by

$$\overleftrightarrow{\mathbf{T}}(\mathbf{r}_{12})=\frac{e^{ikr_{21}}}{r_{21}}\left[\left[1+\frac{i}{kr_{12}}-\frac{1}{k^2r_{21}^2}\right]\overleftrightarrow{\mathbf{I}}-\left[1+\frac{3i}{kr_{21}}-\frac{3}{k^2r_{21}^2}\right]\hat{\mathbf{r}}_{21}\hat{\mathbf{r}}_{21}\right]\ . \tag{7}$$

In Eq. (7), $\mathbf{r}_{21}=\mathbf{r}_2-\mathbf{r}_1$. In scattering the oscillation dipole is induced by an applied field

$$\mathbf{p}(\mathbf{r}_1)=\overleftrightarrow{\alpha}\cdot\mathbf{E}(\mathbf{r}_1)\ , \tag{8}$$

where $\overleftrightarrow{\alpha}$ is the polarizability tensor.

We now consider scaling arguments for functional dependences for various types of scattering. The dipole tensor has two limiting forms: the near field ($kr_{21}<1$), $T_{21}\sim(kr_{21})^{-2}\exp(-ikr_{21})/r_{21}$, and the far field ($kr_{21}>1$), $T_{21}\sim\exp(-ikr_{21})/r_{21}$. The subscripts represent the position vectors. Single scattering involves scattering to the detector only, hence $E_2\sim k^2T_D\alpha E_1$, where T_D represents the far field tensor scattering to the detector. This is by far the major contributor to I_{VV}, hence $I_{VV}\sim|E_2|^2\sim k^4\sigma I_1$, where I_1 is the incident intensity. The cross section σ involves both the polarizability $\sigma\sim\alpha^2$ and the phase term of the dipole tensor. For forward scattering such that $qR_g<1$, $\sigma\sim N^2a^6$. For $qR_g>1$, $\sigma\sim N^2a^6(qR_g)^{-D_f}\sim Na^{6-D_f}$. Our experiments measured ρ in the forward scattering limit, hence we shall use $I_{VV}\sim k^4N^2a^6I_1$.

The lowest-order multiple scattering and contributor to I_{VH} is double scattering, which involves two successive scattering events; hence $E_3\sim k^2T_{32}\alpha k^2T_{21}\alpha E_1$. For intercluster double scattering T_{32} is T_D, far field to the detector, and T_{21} is also far field, but within the scattering volume. Then we have $I_{VH}\sim k^8\sigma^2I_1$. Scattering at forward angles could involve two successive forward scatterings, hence $\sigma^2\sim(N^2a^6)^2$; two successive backward scatterings, hence $\sigma^2\sim(Na^{6-D_f})^2$; or anything in between. Given all this and the near forward single scattering, we predict $\rho\sim k^4N^2a^6$ to $k^4a^{6-2D_f}$.

Intracluster double scattering involves a near field scattering within the cluster, because $kr_{21}<1$ for a typical cluster size, followed by a far field scattering to the detector, hence $E_3\sim k^2T_D\alpha k^2r_{21}^{-1}(kr_{21})^{-2}\alpha' E_1\sim k^2T_D\alpha\langle r_{21}^{-3}\rangle\alpha' E_1$. Note the cancellation of a second power of k. The $\langle r_{21}^{-3}\rangle$ indicates an average over all pairs of monomers and since r_{21} is the monomer center to center distance it should scale as a^{-3}. We have also written α' to represent the monomer polarizability. It follows that $I_{VH}\sim k^4\sigma a^{-6}\sigma' I_1$, where σ' is the monomer cross section which we take to be in the Rayleigh regime $ka<1$, thus $\sigma'\sim a^6$. For forward scattering $\sigma\sim N^2a^6$, to yield $I_{VH}\sim k^4a^6I_1$, where we have left out an unknown N dependence. Ratioing this with the single scattering result we find that ρ does not have a dependence on k or a when the scattering is intracluster. A summary of the results of these scaling arguments is given in Table I.

We measured the wavelength dependence of ρ for our

TABLE I. Results of scaling arguments for functional dependences of the depolarization ratio of light scattered from aggregates with $D_f=1.8$.

Type of scattering	Wavelength	Monomer size	Monomer per cluster	Scattering volume
Intercluster	λ^4	$a^{2.4}$–a^6	N^0–N^2	V_s
Intracluster	λ^0	a^0	undetermined	V_s^0

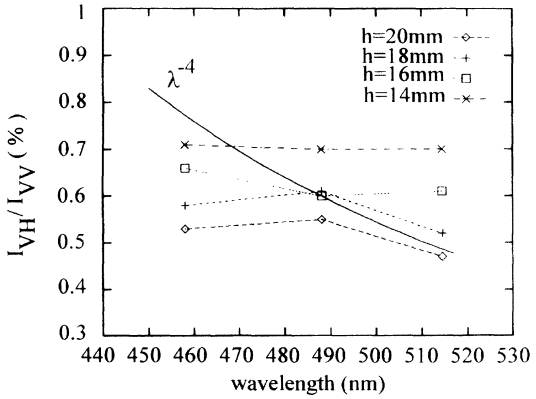

FIG. 1. The depolarization ratio versus incident wavelength at several different heights above burner. The line indicates a λ^{-4} dependence.

flames by using three lines available in the argon ion laser, $\lambda=458$, 488, and 514.5 nm. Although this is not a large range, we are looking for a fourth power dependence which should be easily detected. Figure 1 shows our results. No wavelength dependence was seen, which strongly supports the intracluster scenario.

Our main results are shown in Fig. 2. Here we plot the depolarization ratio at small θ such that $qR_g \ll 1$ for three different flames as a function of the mean number of monomers per aggregate. Recall that this latter parameter was also determined by *in situ* light scattering and has been corrected for polydispersity. All three flames yield a universal dependency of ρ on N, which we find to be a power law

$$\rho \sim N^{-x} \tag{9}$$

with $x=0.6\pm0.1$. Since $qR_g \ll 1$, $I_{VV} \sim N^2$; thus our results imply $I_{VH} \sim N^{1.4}$. These functional dependences once again argue against intercluster multiple scattering as the cause of the depolarization since our arguments above had implied $\rho \sim N^0 - N^2$ for this type of scattering.

This functional dependence can also argue against anisotropy as the cause for the depolarization, although the argument is not conclusive. For simulated DLCA clusters it has been shown that the anisotropy, as measured by the ratio of the maximum to minimum principle values of the radius of gyration tensor, is not a function of N [26,27]. The depolarization ratio predicted by Mie theory due to anisotropy of spheroids, however, is a function of anisotropy. If spheroids and cluster behave similarly in this manner, then the $\rho - N^{-0.6}$ dependency is not due to anisotropy.

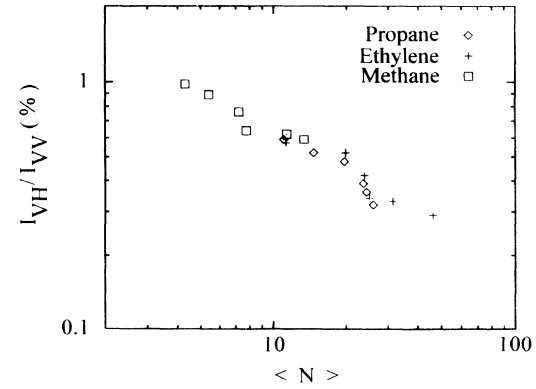

FIG. 2. The depolarization ratio versus average number of monomers per aggregate $s_1 = \langle N \rangle$ for three different flames.

IV. DEPOLARIZATION FOR SIMULATED FRACTAL AGGREGATES

To understand our results further we have calculated the depolarization ratio for light scattered from computer generated fractal aggregates. The simulation we used was similar to that described in [28] to create DLCA clusters. The simulation was in three dimensions and off lattice and yielded clusters with a fractal dimension of $D_f = 1.75 \pm 0.10$.

To calculate the scattering the applied field at any given monomer was taken as due to the incident field plus all the fields scattered from the other monomers. This was solved in an iterative self-consistent manner. The monomer scattering was taken as due to the electric dipole, hence Eqs. (6)–(8) were used. Thus we have a self-consistent electric-dipole-induced-dipole calculation. We used $\lambda=488$ nm and $ka=0.2$, hence a monomer radius of $a=15.5$ nm, a typical value for soot. We also used a complex refractive index $m=1.6-0.61$, again typical of soot.

Before we compare to our data, we use our scheme to calculate ρ for linear arrangements of N monomers. For $N=3$ this allows a comparison to the results of Jones [16]. We calculated ρ for 204 different orientations of the linear clusters using equally spaced Eulerian angles. The results compared to Jones are shown in Table II, where the comparison is seen to be very good. Figure 3 shows ρ vs N for orientationally averaged linear clusters. This shows ρ increases monotonically with N unlike our experimental results for fractal clusters.

The calculation of ρ for the DLCA fractal clusters was performed for clusters of $N=3$, 11, 19, 28, 42, 52, 78, and 98, again averaged over 204 orientations. The results are

TABLE II. Comparison of our self-consistent, electric-dipole-induced-dipole calculation for orientationally averaged, linear chains of $N=3$ spherical monomers to the results of Jones [16] for the depolarization ratio at $\theta=0°$ and $ka=0.2$, where a is the monomer radius for various refractive indices m.

m	Jones Ref. [16]	This work
1.4	1.26	1.24
1.4–0.5i	3.39	3.40
1.5	1.89	1.84
1.5–0.5i	3.93	3.91
1.6	2.60	2.55
1.6–0.5i	4.55	4.53

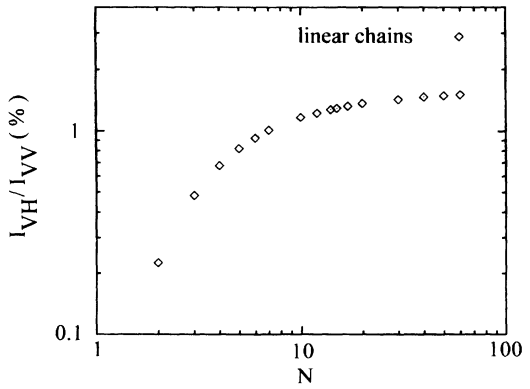

FIG. 3. The depolarization ratio versus number of monomers per aggregate for linear chains. $m = 1.6-0.6i$ and $ka = 0.2$.

shown in Fig. 4, which shows a very large degree of cluster to cluster variation even after orientational averaging. This large variation has been noted before [13]. Averaging over clusters of the same N, however, brings some order out of this chaos and a fit to these averages yields $\rho \sim N^{-x}$, $x = 0.6 \pm 0.1$, in excellent agreement with our experimental results in Fig. 2. We conclude that electric-dipole-induced-dipole intracluster scattering is the source of the depolarized scattering in our fractal soot aggregates.

Frey *et al.* [18] also calculated ρ and I_{VH} for fractal aggregates with $16 \leq N \leq 512$ and $D_f = 1.0$, 1.5, 1.9, and 3. Among their conclusions was $I_{VH} \sim N^{2-2/D_f}$. For our $D_f \approx 1.8$, this yields $N^{0.9}$, in disagreement with our experimental result of $I_{VH} \sim N^{1.4}$. However, their simulated data do not agree with their exponent of $2-2/D_f$, but rather we find by fitting their data $I_{VH} \sim N^{1.2}$, in approximate agreement with our experiment.

With the correct functional dependence, we now attempt to obtain quantitative agreement between experiment and simulation. As described above, the average number of monomers per aggregate was determined from the light scattering assuming the size distribution of clusters was given by the scaling results, Eqs. (5). Then to compare our calculations to experiment we must calculate ρ for an ensemble of simulated clusters weighted according to Eqs. (5) with the same average sizes as for the data. As described above, we have calculated $\rho(N)$ for only eight different N values, not for every consecutive size. We can still find a weighted average for ρ, however, with the $\rho(N)$ values available by multiplying by the $n(N)$ values for a given available N and $\langle N \rangle$ given by Eqs. (5) and then normalizing with only those $n(N)$ values. We have done this, and the results are shown in Fig. 5. We see once again the correct N dependence, but ρ from the calculation is about a factor of 8 too small.

Why the discrepancy? The answer has more than one part. First, consider the intracluster, near field scattering with an r^{-3} distance dependence. This implies the intermediate scattered field varies rapidly with distance and the field at the center of a given spherical monomer due to scattering from a nearby monomer is not the average field over the volume of the receiving monomer. To correct this we have calculated the average field scattered to a given monomer during the intermediate intracluster scattering and used it rather than the field at the center. This correction yields a value of ρ greater by a factor of about 2 than the nonaveraged calculations as shown in Fig. 5. The agreement with experiment is now better, but still unsatisfactory. We remark that field averaging applied to the linear $N = 3$ chain would also increase ρ and the agreement in Table II with Jones would then disappear. Obviously approximating the field over the monomer as the field at the center is not valid.

A source of error in describing a real cluster is the nonpoint contacts, or necking between monomers in real soot clusters. The thickness of this necking bridge often approaches the size of the monomers. Simulated clusters have no necks between monomers. What effect might necking have on ρ?

This question is difficult to answer because the degree

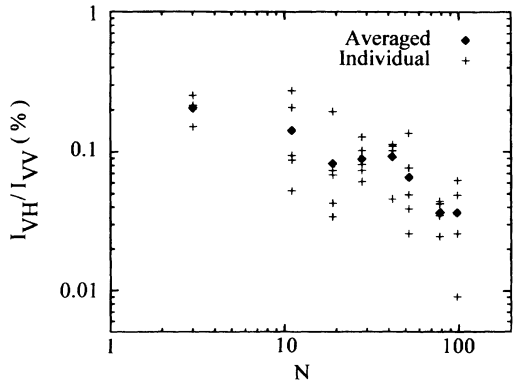

FIG. 4. The depolarization ratio versus number of monomers per aggregate for computer generated DLCA clusters. Results for individual clusters of a given N are orientationally averaged yet show significant variation. Also shown are averages for several clusters of each N.

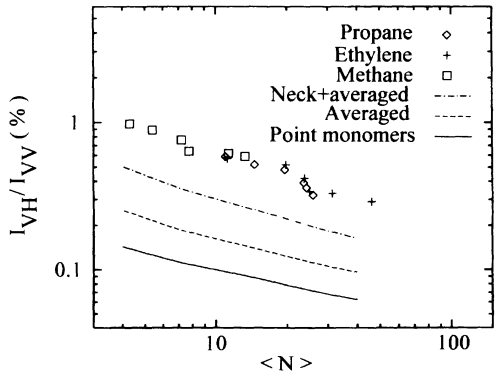

FIG. 5. Comparison of the flame data for depolarization ratio versus average number of aggregates per cluster and calculation. The solid line is for no field averaging and no necking, the dashed line is for field averaging over the monomer and no necking, and the dot-dashed line is for both field averaging and necking.

of necking is hard to quantify and there is no theory for light scattering for such an unusual geometry. We can, however, make a qualitative overestimate of the effect of necking on ρ by temporarily replacing each monomer doublet in a simulated cluster with a prolate spheroid of 2:1 aspect ratio. The total dipole moment for the spheroid is calculated using known electromagnetic theory and then divided in two, each half now representing the dipole moment of the two individual monomers. This then represents the scattered field due to nearest neighbors with extreme necking. With this start, the self-consistent dipole-induced-dipole calculation proceeds as before. We consider this an overestimate because the prolate spheroid is an extreme representation of necking between two spherical monomers. Again in Fig. 5 we show the combined effect of the field averaging and necking corrections. Agreement is improved, but still discrepancy exists in overall magnitude.

The monomer size is not a relevant factor in ρ. Our scaling arguments summarized in Table I indicated no dependence of ρ on the monomer radius for intracluster scattering. We have tested this with our calculation and show the results for the field averaged, no neck situation in Fig. 6 and indeed find only a weak dependence.

Further modifications can be made to change the comparison between experiment and calculation. Both are sensitive to the value of τ, the exponent in the scaling size distribution, Eqs. (5). We picked $\tau=0$ in this work because then Eqs. (5) are consistent with the simulations of Graham and Robinson [29] for coalescent aggregation in the free molecular regime. The soot is in the free molecular regime, but is obviously not coalescent. Fractal aggregation in the free molecular regime is complex and values of τ as large as $\frac{2}{3}$ have been estimated. We are currently working on this problem experimentally and preliminarily find $r=0.2\pm0.2$.

The soot refractive index m is also an important factor for ρ and the experiment versus calculation comparison changes with this parameter. This opens the exciting possibility of an *in situ* refractive index measurement using ρ, and we are currently pursuing this opportunity. Indeed a good match between experiment and calculation can be achieved by adjusting with τ and m, but we feel it is too soon to make any quantitative conclusions regarding such a match.

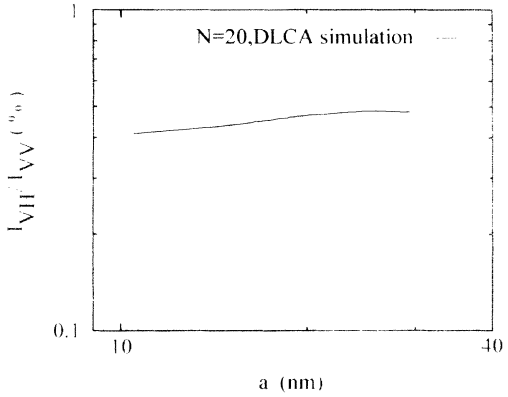

FIG. 6. Depolarization ratio dependence on monomer size for $N=20$.

V. CONCLUSION

We conclude that fractal aggregates of modest size experience intracluster multiple scattering. The size dependence is $\rho\sim N^{-0.6}$. The intracluster scattering is controlled by the near field term of the electric dipole scattering tensor. The field at each monomer should not be approximated as uniform and equal to the field at the monomer center even for our Rayleigh-like size parameter of $ka=0.2$. The magnitude of ρ is sensitive to a number of details of the cluster morphology, optical properties, and size distribution, but there is a good possibility that the refractive index may be determinable from ρ. Furthermore, bolstered by our success in describing ρ theoretically, we can now approach the multiple scattering problem with the goal of accurately understanding both scattering and absorption by fractal aggregates so common in our environment.

ACKNOWLEDGMENTS

We thank J. Cai for useful collaboration. This work was supported by NSF Grant No. CTS9024468.

[1] F. Family and D. P. Landau, *Kinetics of Aggregation and Gelation* (North-Holland, Amsterdam, 1984); D. W. Schaefer, J. E. Martin, P. Wiltzius, and D. S. Cannell, Phys. Rev. Lett. **52**, 2371 (1984); T. Freltoft, J. K. Kjems, and S. K. Sinha, Phys. Rev. B **33**, 269 (1986).

[2] A. J. Hurd and W. L. Flower, J. Colloid Interface Sci. **122**, 178 (1988).

[3] H. X. Zhang, C. M. Sorensen, E. R. Ramer, B. J. Olivier, and J. F. Merklin, Langmuir **4**, 867 (1988).

[4] S. Gangopadhyay, I. Elminyawi, and C. M. Sorensen, Appl. Opt. **30**, 4859 (1991).

[5] C. M. Sorensen, J. Cai, and N. Lu, Appl. Opt. **31**, 6547 (1992).

[6] C. M. Sorensen, J. Cai, and N. Lu, Langmuir **8**, 2064 (1992).

[7] J. Cai, N. Lu, and C. M. Sorensen, Langmuir **9**, 2861 (1993).

[8] M. V. Berry and I. C. Percival, Opt. Acta **33**, 577 (1986).

[9] J. Nelson, J. Mod. Opt. **36**, 1031 (1989); Nature **339**, 611 (1989).

[10] J. de Ris, in *Seventeenth Symposium (International) on Combustion* (The Combustion Institute, Pittsburgh, 1978), p. 1003.

[11] D. J. Lien, in *Comets in the Post-Halley Era*, edited by R. L. Newburn *et al.* (Kluwer, Dordrecht, 1991), Vol. 2, p. 1005.

[12] Z.-Y. Chen, P. Weakliem, W. Gelbart, and P. Meakin, Phys. Rev. Lett. **58**, 1996 (1987).

[13] G. Seeley, T. Keyes, and T. Ohtsuki, Phys. Rev. Lett. **60**, 290 (1988).

[14] M. Lax, Rev. Mod. Phys. **23**, 287 (1951); D. S. Saxon, Phys. Rev. **100**, 1771 (1955); V. Twersky, J. Math. Phys. **8**,

589 (1967); J. C. Ravey, J. Colloid Interface Sci. **46**, 139 (1974).
[15] C. M. Sorensen, R. C. Mockler, and W. J. O'Sullivan, Phys. Rev. A **14**, 1520 (1976); **17**, 2030 (1978).
[16] A. R. Jones, J. Phys. D **12**, 1661 (1979).
[17] Z. Chen, P. Sheng, D. A. Weitz, H. M. Lindsay, M. Y. Lin, and P. Meakin, Phys. Rev. **37**, 5232 (1988).
[18] J. Frey, J. J. Pinvidic, R. Botet, and R. Jullien, J. Phys. (Paris) **49**, 1969 (1988).
[19] S. R. Forrest and T. A. Witten, J. Phys. A **12**, L109 (1979).
[20] A. D'Alessio, A. DiLorenzo, A. F. Sarafim, F. Berretta, S. Masi, and C. Venitzaai, in *Fifteenth Symposium (International) on Combustion* (The Combustion Institute, Pittsburgh, 1975), p. 1427; A. D'Alessio, in *Particulate Carbon,* edited by D. C. Siegla and G. W. Smith (Plenum, New York, 1981), p. 207.
[21] B. M. Vaglieco, F. Beretta, and A. D'Alessio, Comb. Flame **79**, 259 (1990).
[22] J. Cai, N. Lu, and C. M. Sorrensen (unpublished).
[23] P. G. van Dongen and M. H. Ernst, Phys. Rev. Lett. **54**, 1396 (1985).
[24] B. S. Haynes and H. Gg. Wagner, Ber. Bunsenges, Phys. Chem. **84**, 585 (1980).
[25] C. E. Bohren and D. R. Huffman, *Absorption and Scattering of Light by Small Particles* (Wiley, New York, 1983).
[26] F. Family, T. Viscek, and P. Meakin, Phys. Rev. Lett. **55**, 641 (1985).
[27] R. Botet and R. Jullien, J. Phys. A **19**, L907 (1986).
[28] P. Meakin, J. Colloid Interface Sci. **102**, 491 (1984); **102**, 505 (1984); Phys. Lett. **107A**, 269 (1985).
[29] S. C. Graham and A. Robinson, J. Aerosol Sci. **7**, 261 (1976).